GEOPHYSICAL RESEARCH LETTERS, VOL. 28, NO. 7, PAGES 1203-1206, APRIL 1, 2001

Lidar Observations of Polar Mesospheric Clouds at South Pole: Seasonal Variations

Xinzhao Chu, Chester S. Gardner, and George Papen

Department of Electrical & Computer Engineering
University of Illinois at Urbana-Champaign, Illinois, USA

Abstract. Polar mesospheric clouds (PMCs) were observed above the geographic South Pole by an Fe Boltzmann temperature lidar from 11 Dec 99 to 24 Feb 00. During this 76-day period 297 h of observations were made on 33 different days and PMCs were detected 66.5% of the time. The mean PMC peak backscatter ratio, peak volume backscatter coefficient, total backscatter coefficient, layer centroid altitude, and layer rms width are 50.59 ± 2.33, 2.70 ± 0.12×10^{-9} $m^{-1}sr^{-1}$, 3.61 ± 0.22×10^{-6} sr^{-1}, 85.49 ± 0.09 km, and 0.71 ± 0.03 km, respectively. The PMCs are highest near summer solstice when upwelling over the pole is strongest. The altitudes are 2-4 km higher than that typically observed elsewhere, including the North Pole. After solstice the mean altitudes decreases by about 64 m/day as the upwelling weakens.

Introduction

Polar mesospheric clouds (PMCs) occur in the mesopause region at high latitudes during mid-summer when temperatures fall below about 150 K. Noctilucent clouds (NLCs) are the visual manifestation of PMCs that are seen only at night when the mesopause region is still sunlit. PMCs/NLCs are usually observed poleward of 50° in both hemispheres. During the past two decades much has been learned about NLCs, PMCs and the related Polar Mesospheric Summer Echo (PMSE) phenomenon. Extensive lidar, radar, rocket, and satellite observations in the Northern Hemisphere have characterized the altitude distribution, geographic extent, and scattering properties of PMCs and PMSEs. Several excellent reviews of PMC/NLC/PMSE characteristics and the current understanding of their formation mechanisms can be found in *Gadsden and Schröder* [1989], *Thomas* [1991; 1994], *Avaste* [1993], and *Cho and Röttger* [1997].

The lack of Southern Hemisphere sightings of NLCs is due in part to the scarcity of observers in the critical latitude range. Most of the observations of PMC/NLC in the Southern Hemisphere have been made by satellites [e.g., *Thomas and Olivero*, 1989; *Debrestian et al.*, 1997; *Carbary et al.*, 1999]. Recent radar observations at high southern latitudes have shown that PMSEs are weaker and more sporadic than their Northern Hemisphere counterparts [*Balsley et al.*, 1995; *Huaman and Balsley*, 1999]. Satellite and in situ rocket data indicate that the summer mesopause temperatures are a few degrees warmer in the Southern Hemisphere than in the north [*Huaman and Balsley*, 1999; *Lübken et al.*, 1999], which may explain the PMSE differences. However, SME satellite observations of PMCs in both hemispheres reveal similar geographic and seasonal variations [*Thomas and Olivero*, 1989]. Although NLC/PMC have been well characterized in the north, progress in understanding the hemispherical differences are exacerbated by the lack of direct observations over Antarctica. In this paper we report the first lidar observations of PMCs at South Pole. The data were obtained throughout the 1999-2000 austral summer and are used to characterize the seasonal variations in the PMC structure.

Paper number 2000GL012524.
0094-8276/01/2000GL012524$05.00

Fe Lidar System

The observations were made by the University of Illinois Fe Boltzmann temperature lidar at 372 and 374 nm. The system was designed to measure temperatures from 30-80 km using the Rayleigh technique and in the mesopause region using the Fe Boltzmann technique [*Gelbwachs*, 1994]. The lidar includes two frequency-doubled, injection-seeded alexandrite lasers operating at about 3 W each in the UV and two 0.4 m diameter telescopes. To minimize background noise from solar scattering in the atmosphere, the divergence of each laser beam and the field-of-view of each telescope are limited to 0.5 mrad full-width and the detector channels include narrowband interference filters and Fabry-Perot etalons. The optical bandwidth of the detectors is 30 GHz full-width-at-half-maximum (FWHM).

Normally the system is operated with the lasers tuned to the 372 and 374 nm Fe resonance lines. The 374 nm line is an upper state whose population is determined by the temperature dependent Boltzmann factor. The ratio of the backscattered Fe signals on these two lines is a sensitive function of temperature [*Gelbwachs*, 1994]. Fe chemistry is temperature dependent. The primary sink reaction FeO + $O_2 \rightarrow FeO_3$ on the layer bottom side proceeds most rapidly at low temperatures [*Rollason and Plane*, 2000]. For most of the summer, very little Fe exists below 90 km because of the extremely cold mesopause. Consequently, it was not possible to measure the temperature near the PMCs. However, a small amount of Fe may exist in the 82-86 km region where PMCs are typically observed. The 374 nm Fe signals are a factor of 20-30 weaker than the 372 nm Fe signals while the PMC signal levels are comparable. Typically the Fe signal at 374 nm is less than 1% of the peak PMC signal. Even so, during routine observations, both lasers were periodically tuned off the Fe resonance line by 10 GHz to confirm the presence of PMCs. To minimize contamination by weak Fe scattering, PMC parameters were derived primarily from the 374 nm data. The 372 nm data were used to determine the altitude and occurrence probability of the PMCs only if 374 nm data were unavailable. All of the data reported here were obtained with a vertical resolution of 48 m and then

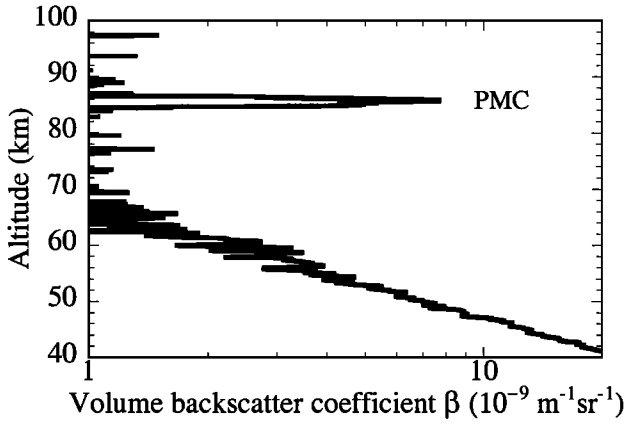

Figure 1. Volume backscatter coefficient profile of PMC and molecular scattering versus altitude obtained between 2238-2300 UT on 18 Jan 00.

were smoothed using a 250 m FWHM Hamming window. The PMC parameters are computed from the lidar profiles using the approach described in *Chu et al.* [2001].

Observations

The Fe lidar was installed in the Atmospheric Research Observatory 488 m north of the geographic South Pole in Nov 99. Observations began on 02 Dec 99. The first PMC scattering layers were detected on 11 Dec 99 and the last were observed on 24 Feb 00. During the 76-day period from 11 Dec through 24 Feb, 297 h of lidar data were collected on 33 different days. PMCs were observed 66.5% of the time during this period. This is comparable to the seasonal averaged occurrence frequency of 60% for 90°S derived from 1981-85 SME satellite data by *Thomas and Olivero* [1989]. *Von Zahn et al.* [1998] reported an occurrence frequency of 46% for lidar observations at Andoya (69°N). The Andoya and South Pole lidar observations are consistent with the SME data, which showed much higher PMC occurrence frequencies above 80°, compared to those below 70°.

Plotted in Figure 1 is the volume backscatter coefficient profile obtained between 2238-2300 UT on 18 Jan 00. It was computed by combining the 372 and 374 nm profiles obtained with both lasers tuned off the Fe resonance lines. The thin layer near 85.7 km is the PMC. The peak PMC signal is comparable to the range corrected molecular scattering at about 48.7 km. The peak aerosol backscatter ratio for this PMC is 144.

The PMC peak backscatter ratio R_{max}, peak volume backscatter coefficient β_{max}, total backscatter coefficient β_{Total}, layer centroid altitude Z_C, and layer rms width were derived from the hourly mean profiles. These data (except rms width) and PMC occurrence probability are plotted versus day number relative to summer solstice (21 Dec 99) in Figure 2. Data from the 372 nm channel are plotted in Figures 2d and 2e only when 374 nm data are not available (73 h out of 297 h). The large variations in these parameters are associated with the strong diurnal oscillations [*Chu et al.*, 2001]. In addition, the centroid altitude exhibits a seasonal trend, which may be associated with strong upwelling over the summer polar cap. The smooth dashed curve is a fourth order polynomial fit to all the 374 nm centroid altitude data. The solid line is a linear fit to the 374 nm

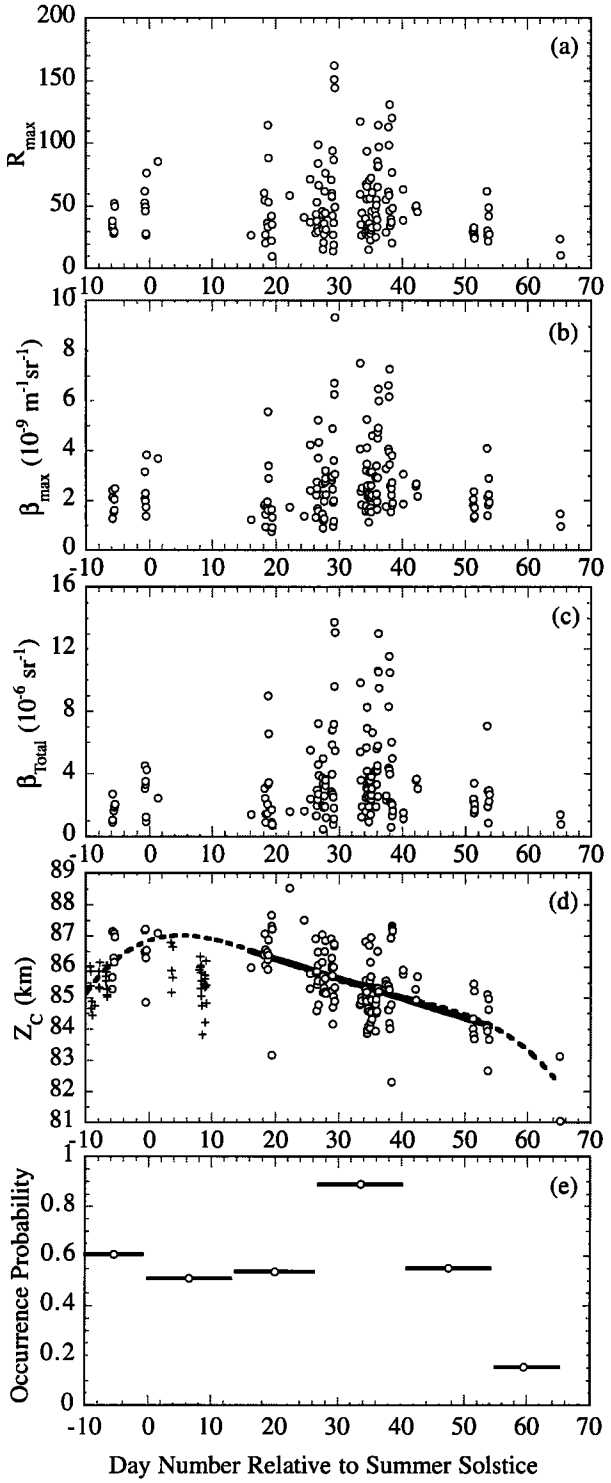

Figure 2. Seasonal variation of the hourly mean PMC (a) peak backscatter ratio, (b) peak volume backscatter coefficient, (c) total backscatter coefficient, (d) centroid altitude, and (e) PMC occurrence probability plotted versus day number relative to austral summer solstice (21 Dec 99). The open circles are the data from 374 nm lidar channel while the crosses are the data from 372 nm lidar channel. In Figure 2d, the dashed line is the 4^{th} order polynomial fit to all the 374 nm data, while the solid line is the linear fit to the 374 nm data between day 18 and day 53. The linear fit equation is Z_C(km) = 87.54 - 0.064 Day, i.e., the slope is 64 m/day.

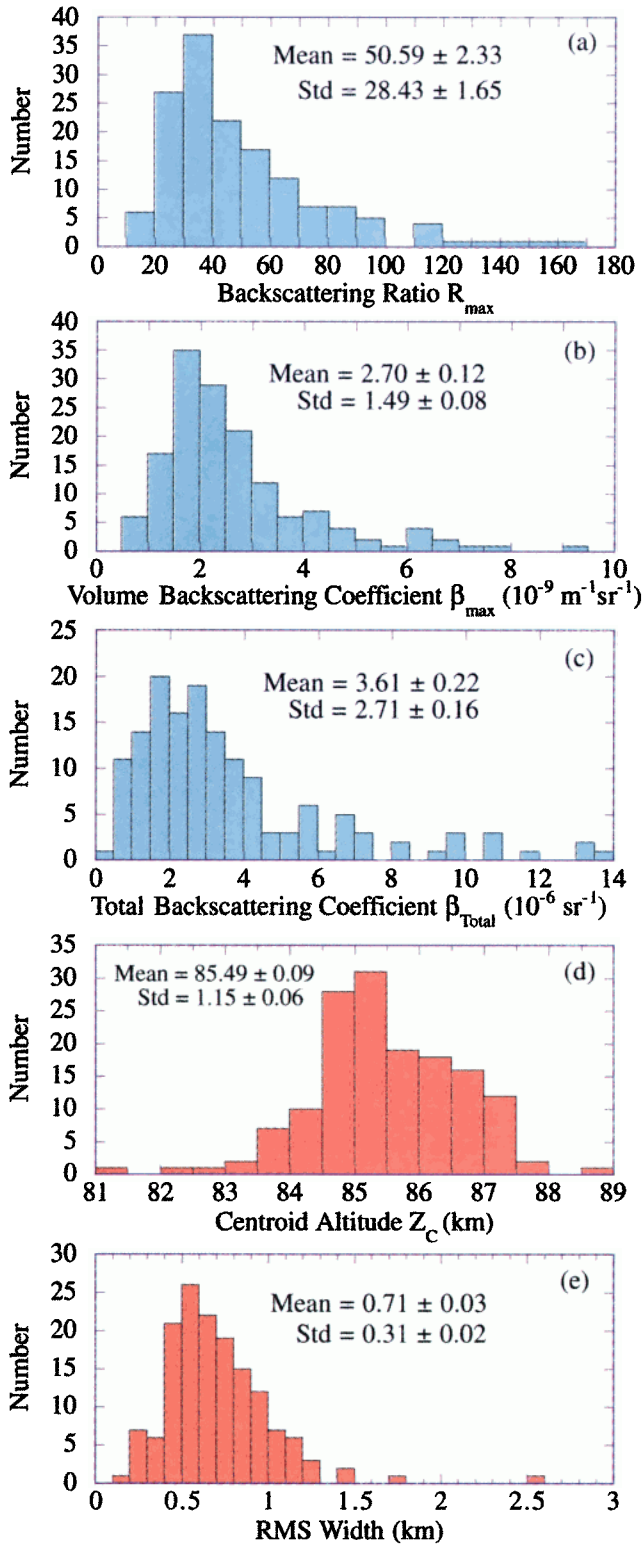

Figure 3. Histograms of PMC characteristics at South Pole in the 99-00 austral summer season derived from 149 h of 374 nm lidar data. (a) Peak backscatter ratio, (b) peak volume backscatter coefficient, (c) total backsscatter coefficient, (d) layer centroid altitude, and (e) layer rms width.

data obtained from day 18 to 53. The fit suggests that the centroid altitude is highest near solstice when the upwelling associated with the diabatic circulation system is strongest [*Garcia and Solomon*, 1985], and then decreases by about 64 m/day after solstice as the upwelling weakens. *Chu et al.* [2001] and *von Zahn et al.* [1998] reported strong 12 and 24 h oscillations in the PMC altitude and backscatter ratio, which were attributed to a few cm/s oscillations in the vertical winds. The oscillation velocities are comparable to the maximum upwelling velocities expected during the observation period. The PMC backscatter parameters and occurrence probability all exhibit maxima 30-40 days after solstice and then decrease rapidly towards the end of summer. This is qualitatively consistent with satellite observations [*Thomas and Olivero*, 1989].

Histograms of the PMC peak backscatter ratio, peak volume backscatter coefficient, total backscatter coefficient, layer centroid altitude, and layer rms width derived from the 149 h of 374 nm data in which PMCs were detected are shown in Figure 3. The mean rms width of South Pole PMCs is 0.71 ± 0.03 km. This value is comparable to Northern Hemisphere measurements. The PMC centroid altitude was above 85 km 66.4% of the time. The mean altitude of 85.49 ± 0.09 km is significantly higher (2-4 km) than that reported from the Northern Hemisphere or from satellite observations. Numerous observations in the Northern Hemisphere show that the typical altitude of PMCs is between 82-83 km. For example, the mean altitude of NLCs observed at 54.63°N is 83.4 km [*von Cossart et al.*, 1996]; the mean altitude of NLCs observed at 69°N is 82.7 km [*von Zahn et al.*, 1998]. But *Hecht et al.* [1997] observed NLCs between 84 and 86 km at 67°N in Sondrestrom, Greenland. The mean NLC altitudes in the Southern Hemisphere, deduced from POAM II satellite measurements by *Debrestian et al.* [1997], are between 82-83 km. *Carbary et al.* [2000] found the mean altitude of PMCs over Antarctica is 82.3 km. *Thomas and Olivero* [1986] used SME satellite data to determine that the PMC cloud altitudes in the Northern Hemisphere (85.0 ± 1.5 km) are about 2 km higher than in the Southern Hemisphere. Our lidar observations contradict this result.

The mean peak backscatter ratio R_{max} of South Pole PMCs is 50.59 ± 2.33, which is comparable to the value obtained by *von Zahn et al.* [1998], but almost half of the value (98 ± 2.5) obtained by *von Cossart et al.* [1999]. This is consistent with the reduced albedo of PMC observed by satellites over the southern Polar Regions compared to the north [*Thomas and Olivero*, 1989]. The mean peak volume backscatter coefficient β_{max} of the South Pole PMCs is 2.70 ± 0.12×10^{-9} $m^{-1}sr^{-1}$, which is a little higher than that reported by *von Cossart et al.* [1999]. The maximum total backscatter coefficient recorded in our South Pole data is 13.75×10^{-6} sr^{-1}, the minimum is 0.48×10^{-6} sr^{-1}, and the mean is 3.61 ± 0.22×10^{-6} sr^{-1}. The PMCs observed at the South Pole belong to the strongest classes according to the computed classification for NLC displays listed in *Meriwether et al.* [1993].

Conclusions

PMCs were observed above the South Pole during the 76-day period from 11 Dec 99 to 24 Feb 00. Almost 300 h of lidar observations were made on 33 different days dur-

ing this period and PMCs were observed 66.5% of the time. The mean peak backscatter ratio 50.59 ± 2.33 is about half the value reported by *von Cossart et al.* [1999] for observations at Andoya (69°N). The most interesting observation is that PMC altitudes recorded by our lidar are about 2-4 km higher than other observations in the Northern Hemisphere. The mean altitude is 85.49 ± 0.09 km compared to 82-83 km typically observed elsewhere. We believe this difference is due in part to the stronger summertime upwelling directly over the South Pole compared to lower latitudes. However, lidar measurements by our group near the North Pole close to summer solstice showed PMCs at altitudes several km lower than at South Pole [*Gardner et al.*, 2001]. These results suggest there might be a significant hemispherical difference in PMC altitudes. The altitude observations reported here contradict previously reported satellite measurements, which suggest that PMCs are about 2 km higher in the Northern Hemisphere [*Thomas and Olivero*, 1986].

We are aware that the results presented in this paper are based on only one summer season of observations and this could bias the statistics. The Fe lidar will be operated for three more summer seasons at the South Pole to improve our statistics of PMC characteristics and to further explore the apparent hemispherical differences in PMC altitudes and scattering ratios.

Acknowledgments. The authors gratefully acknowledge Dr. John Walling and his colleagues at Light Age, Inc., and the staff of Amundsen-Scott South Pole Station for their superb support. We also thank Weilin Pan and Ashraf El Dakrouri for helping to install and operate the lidar system at South Pole. This project was supported by National Science Foundation grants NSF ATM 96-12251 and NSF OPP 96-16664.

References

Avaste, O., Noctilucent clouds, *J. Atmos. Terr. Phys., 55,* 133-143, 1993.

Balsley, B. B., *et al.*, On the lack of Southern Hemisphere polar mesospheric summer echoes, *J. Geophys. Res., 100,* 11685-11693, 1995.

Carbary, J. F., *et al.*, Altitudes of polar mesospheric clouds observed by a middle ultraviolet imager, *J. Geophys. Res., 104,* 10089-10100, 1999.

Cho, J. Y. N., and J. Röttger, An updated review of polar mesosphere summer echoes: Observation, theory, and their relationship to noctilucent clouds and subvisible aerosols, *J. Geophys. Res., 102,* 2001-2020, 1997.

Chu, X., C. S. Gardner, and G. Papen, Lidar Observations of polar mesospheric clouds at South Pole: Diurnal variations, *Geophys. Res. Lett.*, 2001.

Debrestian, D. J., *et al.*, An analysis of POAM II solar occultation observations of polar mesospheric clouds in the Southern Hemisphere, *J. Geophys. Res., 102,* 1971-1981, 1997.

Gadsden, M., and W. Schröder, Noctilucent clouds, *in Physics and Chemistry in Space Planetology,* Vol. 18, Springer-Verlag, New York, 1989.

Garcia, R. R., and S. Solomon, The effect of breaking gravity waves on the dynamics and chemical composition of the mesosphere and lower thermosphere, *J. Geophys. Res., 90,* 3850-3868, 1985.

Gardner, C. S., G. Papen, X. Chu, and W. Pan, First Lidar Observations of Middle Atmosphere Temperatures, Fe Densities and Polar Mesospheric Clouds Over the North and South Poles, *Geophys. Res. Lett.*, 2001.

Gelbwachs, J. A., Iron Boltzmann factor LIDAR: proposed new remote-sensing technique for mesospheric temperature, *Appl. Opt., 33,* 7151-7156, 1994.

Hecht, J. H., J. P. Thayer, D. J. Gutierrez, and D. L. McKenzie, Multi-instrument zenith observations of noctilucent clouds over Greenland on July 30/31, 1995, *J. Geophys. Res., 102,* 1959-1970, 1997.

Huaman, M. M., and B. B. Balsley, Differences in near-mesopause summer winds, temperatures, and water vapour at northern and southern latitudes as possible causal factors for interhemispheric PMSE differences, *Geophys. Res. Lett., 26,* 1529-1532, 1999.

Lübken, F-J., M. J. Jarvis, and G. O. L. Jones, First in situ temperature measurements at the Antarctic summer mesopause, *Geophys. Res. Lett., 26,* 3581-3584, 1999.

Meriwether, J. W., *et al.*, Application of the Rayleigh Lidar to Observations of Noctilucent Clouds, *J. Geophys. Res., 98,* 14979-14989, 1993.

Rollason, R. J., and J. M. C. Plane, The reactions of FeO with O_3, H_2, H_2O, O_2, and CO_2, *Phys. Chem. Chem. Phys., 2,* 2335-2343, 2000.

Thomas, G. E., and J. J. Olivero, The heights of polar mesospheric clouds, *Geophys. Res. Lett., 13,* 1403-1406, 1986.

Thomas, G. E., and J. J. Olivero, Climatology of polar mesospheric clouds 2. Further analysis of Solar Mesosphere Explorer data, *J. Geophys. Res., 94,* 14673-14681, 1989.

Thomas, G. E., Mesospheric clouds and the physics of the mesopause region, *Rev. Geophys., 29,* 553-575, 1991.

Thomas, G. E., Recent developments in the study of mesospheric clouds, *Adv. Space Res., 14,* (9)101-(9)112, 1994.

von Cossart, G., P. Hoffmann, U. von Zahn, P. Keckhut, and A. Hauchecorne, Mid-latitude noctilucent cloud observations by lidar, *Geophys. Res. Lett., 23,* 2919-2922, 1996.

von Cossart, G., J. Fiedler, and U. von Zahn, Size distributions of NLC particles as determined from 3-color observations of NLC by ground-based lidar, *Geophys. Res. Lett., 26,* 1513-1516, 1999.

von Zahn, U., G. von Cossart, J. Fiedler, and D. Rees, Tidal variations of noctilucent clouds measured at 69°N latitude by groundbased lidar, *Geophys. Res. Lett., 25,* 1289-1292, 1998.

X. Chu, C. S. Gardner, and G. Papen, University of Illinois at Urbana-Champaign, 1308 West Main Street, Urbana, IL 61801, USA (email: xchu@uiuc.edu; cgardner@uillinois.edu; g-papen@uiuc.edu)

(Received October 25, 2000; accepted January 12, 2001.)